Laplace- and Diffusion-Field-Controlled Growth in Electrochemical Deposition

P. Garik,[1,2] D. Barkey,[3] E. Ben-Jacob,[1,2] E. Bochner,[1] N. Broxholm,[1] B. Miller,[1] B. Orr,[1] and R. Zamir[1]

[1]*Department of Physics, Randall Laboratory, University of Michigan, Ann Arbor, Michigan 48109*
[2]*Department of Condensed Matter Physics, School of Physics and Astronomy, Tel Aviv University, 69978 Tel Aviv, Israel*
[3]*Department of Chemical Engineering, University of New Hampshire, Durham, New Hampshire 03824*

(Received 7 November 1988)

We distinguish the roles of the Laplace and diffusion fields in electrochemical deposition during growth of the dense-branching morphology. The shape of the growth is controlled by the Laplace field; the microscopic morphology is characteristic of diffusion-field-controlled growth; and the branch size length scale is hypothesized to be the result of the interplay of the two fields. The branching rate varies with system parameters so as to select an apparently constant interfacial velocity.

PACS numbers: 68.70.+w, 05.70.Ln, 64.70.Kb, 81.30.−t

In this paper we study the distinctive roles of the diffusion and Laplace fields in determining the morphological characteristics of the dense-branching morphology[1] (DBM). Many variants of the Hele-Shaw cell have been used to investigate pattern formation in Laplace-field systems,[1-5] while diffusion-field-controlled growth has been studied during solidification from undercooled melts[6,7] and precipitation from supersaturated solutions.[8,9] Our system is electrochemical deposition (ECD) from a binary electrolyte where the electric potential obeys the Laplace equation, while the dynamically established concentration gradient obeys the diffusion equation. Unlike earlier ECD studies,[10-13] we focus on understanding the dynamics of the interplay between the Laplace and diffusion fields by distinguishing the different emergent length scales. This should provide insight into the dynamics of growth of other two-field systems such as diffusion-controlled growth with impurities, directional solidification,[6] and amorphous annealing.[14]

For the parameter range of our study, growth by ECD produces the dense-branching morphology.[1] The DBM is a dimension $d=2$ growth characterized by its branching rate, branch (or finger) thickness, and a stable advancing envelope.[1,15] In our experiments electrodeposition of Cu and Zn, from aqueous $CuSO_4$ and $ZnSO_4$ solutions, respectively, is done at constant voltage, V_0, in quasi-two-dimensional radial Plexiglas cells similar to those described in Refs. 11 and 12. Four distinct length scales emerge during growth. The Laplace-field length scale is the size of the cell. It is evidenced by the determination of the interfacial shape by the anode shape and, for some parameters, by a morphology transition which scales with the cell size. The Laplace field also controls the (Ohmic) current of the cell. The short length scales of the diffusion field and surface tension determine the micron-sized needles and dendrites of the aggregates' branches. Branch thickness is the fourth length scale. It is probably due to the interplay of the Laplace and diffusion fields. This interplay may also have an important role in stabilizing the DBM envelope.

Interfacial growth of the DBM defines a velocity selection problem in terms of the applied driving force, the number of branches, and their thicknesses. Experimentally, we find that as a function of radius the velocity selected by an electrodeposit interface does not simply follow the applied potential; it is apparently constant over much of the cell. This behavior agrees with other DBM velocity measurements.[14,16] Moreover, surprisingly the branching rate adjusts itself so that the selected velocity depends weakly on the electrolyte concentration for a range of parameters.

In our experiment the Laplace and diffusion fields decouple except near the interface. The slowly varying velocity thus allows an independent display of each field's effects. To separate the electrostatic and concentration fields for the binary electrolyte,[17] let $\mathbf{j}_\pm$, $c_\pm$, $\mu_\pm$, $D_\pm$, and $z_\pm$ be the flux, concentration, mobility, diffusion constant, and charge of the (+) cation and (−) anion, respectively. By particle conservation

$$\frac{\partial c_\pm}{\partial t} = -\nabla\cdot\mathbf{j}_\pm = \nabla\cdot(c_\pm\mu_\pm z_\pm F\nabla\phi + D_\pm\nabla c_\pm), \quad (1)$$

with ϕ the electrostatic potential and F the Faraday constant. Assuming charge neutrality outside the interfacial region, substituting $c=c_\pm/\nu_\pm$, with ν_+ (ν_-) the number of cations (anions) per molecule, produces two equations for the electrolyte concentration c. If $D_\pm$ and $\mu_\pm$ are constants, the $\nabla\cdot(c\nabla\phi)$ term cancels to produce $\partial c/\partial t = D\nabla^2 c$, with D an effective diffusion constant. Charge neutrality also implies the Laplace equation $\nabla^2\phi = 0$. In the interfacial region of the aggregate, the ion concentrations couple with the potential through boundary conditions.

Cell construction followed Sawada, Dougherty, and Gollub[11] with the cathode passed through the cell. Cu and Zn cathodes were used for the two respective depositions. The anode was a copper ring seated in the upper and lower plates or a wire seated in a trough. Dissolved impurities influence deposit texture in even ppm concentrations.

© 1989 The American Physical Society

Figure 1(a) is an example of a morphology transition from Cu. Transitions in deposit growth are characterized by (i) a change in color of the deposit from black to red; (ii) a change in branching rate; (iii) a change in the apparent (i.e., visual) density; (iv) a change in slope of the current versus time plot; (v) a change in velocity at the transition point; (vi) a change in the structure on the micron length scale; (vii) a transition occurring between 0.4 and 0.5 of the cell radius, R_0, which varied from 10 to 60 mm; and (viii) a transition interface mimicking the anode shape. The strength of these transition features varies with concentration, cell spacing, and applied potential and may not all concurrently appear. In some cases the black growth has a reddish hue. For the case of a transition with an increase in branching in Cu, features (iii), (vii), and (viii) were reported by Sander and referred to as the Hecker transition.[18] In Fig. 1(a) the circular boundary between the two morphologies coincides with the color transition. Unlike Ref. 18, we find that the morphology transition occurs in Zn, indicating a general field dependence, not a chemical peculiarity to Cu. In Fig. 1(b) Laplace-field boundary conditions show up in the shape of the transition and advancing interfaces for a Zn aggregate grown in a triangular cell. For $CuSO_4$ solutions of $0.025M$, $0.05M$, $0.10M$, the color change from black to red was studied for applied voltages from 2.5 to 30 V; R_0 from 10 to 60 mm; cathode diameters from 0.421 to 3.49 mm; and cell spacings from ≈ 300 to 600 μm. Other morphology transition occurs near the cathode and anode. The color transition is most likely associated with formation of a black layer of cupric oxide, CuO. The layer is thin and rinses off with dilute acid. CuO is unstable at a pH of 4, but can be formed, particularly in the presence of dissolved oxygen, at higher pH because of electrolyte depletion at the interface.[19] The pH values measured for the electrolytes were between 3 and 5 placing the experiment in the range for such oxide formation.

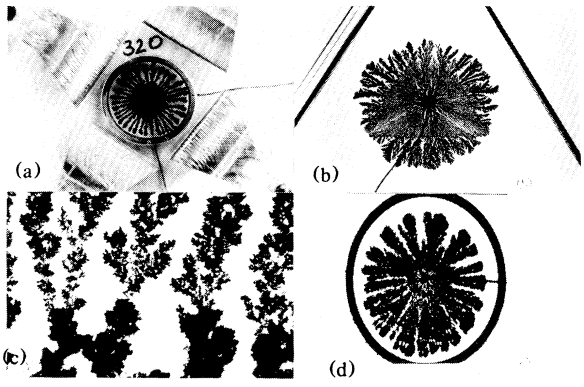

FIG. 1. (a) 5-V growth from $0.10M$ $CuSO_4$ aqueous solution. Spacing of the plates is 290 μm; $R_0=10$ mm. The transition occurs at $R_t \approx 4.4$ mm. The details of the transition are sensitive to cell parameters. (b) Electrodeposition of Zn in a triangular cell from $0.03M$ $ZnSO_4$ solution at 6.0 V and $h_c=435$ μm. The side of the triangle is 80 mm. (c) Transition region at 200×. Growth was from $0.05M$ $CuSO_4$ solution at 5.0 V with $R_0=10$ mm and plate spacing $h_c=290$ μm. (d) A high-resolution-monitor screen dump of the digitized image of an aggregate grown from $0.2M$ $CuSO_4$ solution at 7.5 V. The poor resolution leaves the broad outlines of the branches for comparison to Hele-Shaw fluid flow patterns. The cell is distorted by the imaging (pixel ratio is 1.23:1 in x and y directions).

The Laplace-field length scale, the size of the cell, is demonstrated by the scaling of the morphology transition radius, R_t, with cell size. The scaling of R_t was previously reported by Sander.[18] In the $R_0=40$ mm cell the average R_t is 18 ± 1 mm for V_0 from 5 to 30 V, cell spacings of 290–435 μm, and cathode diameters varying from 0.421 to 3.49 mm. For molarities of $0.025M$, $0.05M$, and $0.10M$ and applied voltages ranging from 5 to 30 V, the transition radius is $\approx 12\pm2$ mm for cell spacing of 435 μm with $R_0=30$ mm and $4.0<R_t<5.0$ mm for $R_0=10$ mm and cell spacing of 290 μm. The transition occurring at a fixed fraction of the cell radius $x_t=R_t/R_0$ cannot be a diffusion-field effect. The distance over which diffusion affects growth can be estimated by the diffusion length $l=D/v$, where v is the interfacial velocity. With $D\approx 9.0\times10^{-6}$ cm^2/sec for $CuSO_4$, and $v\approx 30$ μm/sec, $l\approx 30$ μm. Thus, for diffusion processes the anode is effectively at infinity. Ben-Jacob *et al.* have observed that for the Hele-Shaw cell properties of the $d=2$ Laplace field depend only on $x=r/R_0$, where r is the radius of the interface.[1,15] Specifically, for the Hele-Shaw cell there is an x_c beyond which linear stability analysis predicts the branching will be two dimensional. The transition from fewer to more branches may be the analog result for ECD. In the absence of kinetic effects the predicted x_c for the Hele-Shaw cell is roughly e^{-1} with x_c increasing if kinetic effects are accounted for. The minimum of the current density in a radial cell also occurs at $x=e^{-1}$. It is interesting to speculate that a stability-driven branching transition drives the chemical reaction for the color transition.

The needle growth in Cu and the fine dendritic growth for Zn shown in Figs. 1(a)–1(c) are characteristic of the short length scales of the diffusion field and surface tension interplay. In Fig. 1(b), the pretransition dense clumps appear to be masses of fine needles no greater than 5–10 μm in length, while the post-transition more open branching network has needles about 10–25 μm long. These lengths are comparable to the diffusion length. We expect that the dynamical growth process establishes a concentration gradient on a length scale $\sim l$ about the interface within which diffusional processes dominate morphology selection.

A fourth length scale appears in Fig. 1(d). This low-resolution image of an aggregate emphasizes fingerlike growth reminiscent of the Hele-Shaw cell.[1,3] In contrast to fluid fingering,[20] surface tension in ECD combines

with the diffusion field to determine the micron-scale morphology of needles and dendrites. The interaction of the diffusion and Laplace fields may introduce a new length scale in ECD by generating a region where the concentration varies rapidly. With such a boundary layer we can associate an effective "surface tension" affecting the current distribution at the interface. The finger shapes and the stability of the aggregate's outer envelope are probably a consequence of this boundary layer resulting from the interplay of the Laplace and diffusion fields. The branching shapes at higher voltages [e.g., Fig. 1(a)] are presumably inaccessible in the Hele-Shaw experiment.

To measure the interfacial velocity the image was digitized with a 512×480 pixel grid at intervals of growth. The position of the interface was determined from a radially averaged density profile. Data for runs at $0.2M$ $CuSO_4$ are shown in Fig. 2. The interfacial velocity reaches a constant value 2 mm past the cathode. The selected interface velocity scales with V_0. Assuming only Ohmic currents, if the growth is modeled as a disk of thickness h_a, then in a cell of spacing h_c the interfacial velocity as a function of disk radius r is $v = CV_0/x\ln(1/x)$, where $C = h_c/Zen_m h_a \rho R_0$, Ze is the charge per ion, ρ is the electrolyte resistivity, n_m is the density of the disk, and $x = r/R_0$ is the reduced radius.[21] Since the aggregate's interface, comprised of branch tips, has a smaller surface area than a disk, this computed velocity should be a lower bound. However, as judged by the attempted fits to the data of Figs. 2 and 3, the compound magnitude of C is about 40% too large. This error is independent of voltage and concentration. It suggests either a cell geometry factor or that deposition occurs over a short depth into the aggregate (≈ 50–100 μm). The downturn in v near the anode is probably spurious, arising when more advanced branches cease growing at the anode and reduce the average interface advance. If the magnitude of aggregate resistivity suggested by Grier, Kessler, and Sander[13] is included, this Ohmic model shows a rapid decline for v vs r.

Figure 3(a) shows the velocity signature of the morphology transition at $0.05M$. The data support a flat velocity before and after the transition, although the size of the cell makes confirmation difficult. The jump in velocity is associated with a reduction of branches and interface area at the transition. In Fig. 1(c) the thickness of the pretransition aggregate is 65 ± 10 μm and the posttransition thickness is 72 ± 10 μm. At the transition the thickness is at most 5 μm. The change in interfacial area is less dramatic for $0.1M$ at 5 V; however, a slight increase in velocity is also evident in Fig. 3(b). Use of the average interfacial radius smooths the velocity jump. Studies of single branches under the microscope suggest that the velocity is discontinuous at $0.05M$ and $V_0 = 5$ V. A morphology transition with a discontinuous velocity change as a function of driving force has been characterized as a first-order morphology transition.[15,22] While

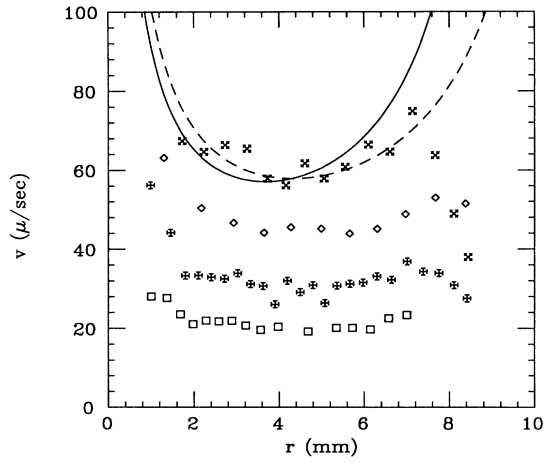

FIG. 2. Interfacial velocity in μm/sec for growth from $0.20M$ $CuSO_4$ aqueous solution. □, 5-V growth; +, 7.5-V growth; ◇, 10-V growth; ×, 12.5-V growth. The solid curve through the 12.5-V data uses the text formula for the velocity with $C = 60\%$ of the computed value. The dashed curve assumes an aggregate resistivity 0.01 that of the electrolyte and larger C. The decrease in velocity for $r > 8$ mm is due to ragged growth: Some branches have reached the anode and stopped growing. Aggregate resolution is 20–25 pixels/mm.

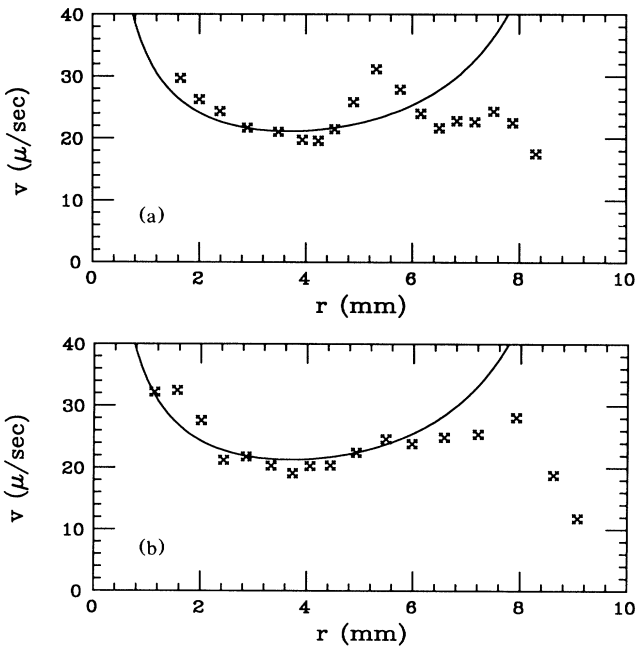

FIG. 3. Interfacial velocity for growth from (a) $0.05M$ and (b) $0.10M$ $CuSO_4$ aqueous solutions at 5 V applied potential. The data for (b) are from Fig. 1(a). The morphology transition for (a) occurs at $R_t \approx 0.46$ mm. The solid curves are computed following the text with 60% of the computed C for each case.

the effective driving force's functional dependence on r here remains to be determined, the transition is at least a generalized example of such a first-order morphology transition.

From Figs. 2 and 3, the selected interfacial velocity at 5 V is nearly independent of electrolyte concentration. Generally we found the aggregate's velocity depended only weakly on concentration.[23] Apparently the branching rate of the DBM is selected so as to attain a specific velocity. For 5 V applied potential, at $0.025M$ and $0.05M$ the pretransition morphology has few branches and is open while the post-transition morphology is dense in branches; at $0.1M$ the morphology is shown in Fig. 1(a); and at $0.2M$ the morphology transition is composed of dense fingers similar to Fig. 1(d). In each case the increase in resistivity at lower molarity is balanced by a change in average density of the aggregate and a decrease in interfacial area.

Above, the importance of the interplay between the Laplace and diffusion fields in determining the aggregate morphology has been emphasized. We conclude that while each field contributes distinctively, with the Laplace field predominant in determining global properties such as shape, an understanding of the interface and its stability must include the interplay of both fields.[24,25]

We thank N. Hecker, R. Goldman, D. Grier, D. Kessler, and J. Broad for valuable conversations and technical assistance. B.O. thanks L. M. Sander for valuable conversations. This research was supported in part by the Donors of the Petroleum Research Fund, administered by the American Chemical Society; the German-Israel Foundation; and National Science Foundation Grant No. DMR-8608305. D.B. acknowledges support from the College of Engineering and Physical Sciences and the Department of Chemical Engineering at the University of New Hampshire. E.B. was supported by the Physics Undergraduate Research Participation Program, Department of Physics, University of Michigan. B.O. acknowledges support by NSF (DMR-8857828).

[1]E. Ben-Jacob, G. Deutscher, P. Garik, N. D. Goldenfeld, and Y. Lareah, Phys. Rev. Lett. **57**, 1903 (1986).

[2]L. Paterson, J. Fluid Mech. **113**, 513 (1981).

[3]E. Ben-Jacob, R. Godbey, N. D. Goldenfeld, J. Koplik, H. Levine, T. Mueller, and L. M. Sander, Phys. Rev. Lett. **55**, 1315 (1985).

[4]G. Daccord, J. Nittmann, and H. E. Stanley, Phys. Rev. Lett. **56**, 336 (1986).

[5]A. Buka and P. Palffy-Muhoray, Phys. Rev. A **36**, 1527 (1987).

[6]J. Langer, Rev. Mod. Phys. **52**, 1 (1980), and references therein.

[7]H. Honjo, S. Ohta, and M. Matsushita, Phys. Rev. A **36**, 4555 (1987).

[8]Y. Sawada, Physica (Amsterdam) **140A**, 134 (1986).

[9]A. Dougherty, P. D. Kaplan, and J. P. Gollub, Phys. Rev. Lett. **58**, 1652 (1987).

[10]M. Matsushita, M. Sano, Y. Hayakawa, H. Honjo, and Y. Sawada, Phys. Rev. Lett. **53**, 286 (1984).

[11]Y. Sawada, A. Dougherty, and J. P. Gollub, Phys. Rev. Lett. **56**, 1260 (1986).

[12]D. Grier, E. Ben-Jacob, R. Clarke, and L. M. Sander, Phys. Rev. Lett. **56**, 1264 (1986).

[13]D. Grier, D. A. Kessler, and L. M. Sander, Phys. Rev. Lett. **59**, 2315 (1987).

[14]G. Deutscher and Y. Lereah, Phys. Rev. Lett. **60**, 1510 (1988); S. Alexander, R. Bruinsma, R. Hilfer, G. Deutscher, and Y. Lereah, Phys. Rev. Lett. **60**, 1514 (1988).

[15]E. Ben-Jacob, P. Garik, and D. Grier, Superlattices Microstruct. **3**, 599 (1987).

[16]Preliminary results for the isotropic Hele-Shaw cell indicate a constant interfacial velocity.

[17]J. Newman, *Electrochemical Systems* (Prentice-Hall, Englewood Cliffs, 1973).

[18]L. M. Sander, in *The Physics of Structure Formation,* edited by W. Güttinger and G. Dangelmayr (Springer-Verlag, Berlin, 1987).

[19]*Atlas of Electrochemical Equilibria in Aqueous Solutions,* edited by M. Pourbaix (Pergamon, Oxford, 1966).

[20]J. V. Maher, Phys. Rev. Lett. **54**, 1498 (1985).

[21]The quantity $Zen_m h_a$ is computed directly as the integrated current between two radii. The experimental setup had a small resistor in series with the electrochemical cell. The resultant change in voltage remained below 5% and does not affect the data analysis.

[22]E. Ben-Jacob, P. Garik, T. Mueller, and D. Grier, Phys. Rev. A **38**, 1370 (1988).

[23]P. Garik, D. Barkey, E. Ben-Jacob, E. Bochner, N. Broxholm, B. Miller, B. Orr, and R. Zamir (to be published).

[24]T. C. Halsey, Phys. Rev. A **36**, 3512 (1987).

[25]D. P. Barkey, R. H. Muller, and C. W. Tobias, J. Electrochem. Soc. (to be published).

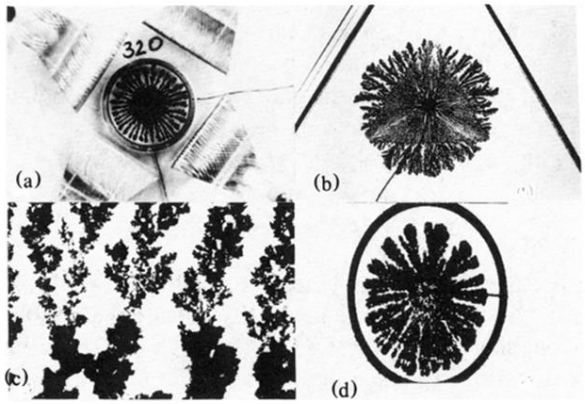

FIG. 1. (a) 5-V growth from 0.10M $CuSO_4$ aqueous solution. Spacing of the plates is 290 μm; $R_0 = 10$ mm. The transition occurs at $R_t \approx 4.4$ mm. The details of the transition are sensitive to cell parameters. (b) Electrodeposition of Zn in a triangular cell from 0.03M $ZnSO_4$ solution at 6.0 V and $h_c = 435$ μm. The side of the triangle is 80 mm. (c) Transition region at 200×. Growth was from 0.05M $CuSO_4$ solution at 5.0 V with $R_0 = 10$ mm and plate spacing $h_c = 290$ μm. (d) A high-resolution-monitor screen dump of the digitized image of an aggregate grown from 0.2M $CuSO_4$ solution at 7.5 V. The poor resolution leaves the broad outlines of the branches for comparison to Hele-Shaw fluid flow patterns. The cell is distorted by the imaging (pixel ratio is 1.23:1 in x and y directions).